Supplementary materials for

Cr(VI) reduction, electricity production, and microbial resistance variation in paddy soil under microbial fuel cell operation

Sections

Table Captions

Figure captions

Fig. S4 pH (A), EC (B) variation curves of soil.

Fig. S5 Changes in soil enzyme activities during SMFC operation (A) Dehydrogenase (B) Urease (C) Invertase (D) Acid Phosphatase.

Fig. S6 Venn diagram on OTU level in different treatments.

Fig. S7 Characterization of electrode materials before and after operation by EDS mapping. (A) EDS image of cathode loaded with Fe_3O_4; (B) EDS image of cathode after the SMFC operation; (C) EDS image of anode microorganisms; (D) EDS image of the anode after SMFC operation.

Section 1: Preparation of cathode supported by Fe_3O_4 catalyst

Cathode preparation: 100×50×3 mm graphite felt (GF) (purchased from Jiangsu Xinye Electronic Materials Factory, Jiangsu, China) was selected as the cathode material of the SMFC, which was ultrasonicated in ethanol for 50 min to remove impurities, removed, and washed. Then put it into an oven and dried at 60℃ for 12 h. It was put into the hydrothermal synthesis reactor and added concentrated nitric acid, and reacted at 90℃ for 9 h. After the reaction was completed, the GF was rinsed continuously with ultrapure water to ensure that the pH of the rinsed water was neutral, and dried at 60℃ for 12 h to complete the pre-activation of the GF. The Fe_3O_4 catalyst was obtained by dissolving 3.6 g of ferric chloride hexahydrate, 6 g of sodium acetate, and 1 g of sodium citrate in 140 ml of ethylene glycol, and repeatedly ultrasonicating for 2 h to form a homogeneous solution. The pre-activated GF was put into a hydrothermal synthesis reactor: the Fe_3O_4 catalyst was added and soaked for half an

hour and then heated at 200℃ for 8 h. After heating, the reactor was cooled down to room temperature, washed repeatedly with ultrapure water and ethanol, and then put into an oven at 60℃ to dry for 12 h. The reaction was then dried at 60℃.

Section 2: Python code of Raspberry Pi voltage acquisition system

```
# -*- coding:UTF-8 -*-
from threading import Timer
import time
import RPi.GPIO as GPIO
import datetime
import os
import sys
import xlwt

sys.path.append('./modules/')

from GetVoltage import get_voltage
from modules.ADS1263 import ADS1263

GPIO.setmode(GPIO.BCM)
CollectTimes = 150

def _get_average_list():
    """smooth"""
    if CollectTimes <= 0:
        print("Error number for the array to averaging!/n")
        return -1
    elif CollectTimes <= 5:
        return sum(VoltageArray) / CollectTimes
    else:
        return sum(VoltageArray) / CollectTimes

# clean txt
book = xlwt.Workbook(encoding='utf-8',style_compression=0)
sheet = book.add_sheet('MFCdata',cell_overwrite_ok=True)
col = ('current time','MFC1','MFC2','MFC3')
for i in range(0,4):
    sheet.write(0,i,col[i])

x=0
while(1):
    x=x+1

    time.sleep(1)

    VoltageArray = []
    for i in range(CollectTimes):
```

```
        VoltageArray.append(get_voltage(0))
    adc1 = _get_average_list()

    ##########################################################

    VoltageArray = []
    for i in range(CollectTimes):
        VoltageArray.append(get_voltage(1))
    adc2 = _get_average_list()

    ##########################################################

    VoltageArray = []
    for i in range(CollectTimes):
        VoltageArray.append(get_voltage(2))
    adc3 = _get_average_list()

    ##########################################################

    curr_time = datetime.datetime.now()
    time_str = datetime.datetime.strftime(curr_time,'%Y-%m-%d %H:%M:%S')

    datalist = [time_str,str(adc1),str(adc2),str(adc3 )]
    print(datalist)

    for j in range(0, 4):
        sheet.write(x, j, datalist[j])
        savepath = '/home/pi/excel.xls'
        book.save(savepath)

    time.sleep(598.5)
```

Section 3: Sampling method

We used a plastic cylindrical straw with a diameter of 0.4 cm and a length of 16 cm as the sediment sampler. The SMFC sediment part is inserted by the sampler vertically at a specific time, and then quickly removed, and the upper, middle, and lower parts of the sampler are mixed as a determination sample. And the fresh sample each time is only 8-16 g, only 0.2-0.4% of the SMFC. The total sampling amount shall not exceed 5% of the total population. Because the sampler is much smaller than SMFC, the disturbance is avoided to a great extent and the normal operation of SMFC is guaranteed.

Section 4: Soil DNA extraction method

Microbial DNA Rapid extraction kit (Shenggong Bioengineering Co., LTD., Shanghai, China) was used to extract total DNA from fresh samples. Specifically, 0.50 g sample, 0.50 g magnetic beads, and 1.0 ml SLX-Mlus Buffer were added in a 2.0 ml Eppendorf tube, and ground for 250 s under 45 HZ. Then added and mixed with 100 μl DS Buffer, and cultivated under 70 ℃ for 10 min and then 90℃ for 2 min. Then the mixture was centrifuged at 10000 g for 5 min at room temperature. 800 μl supernatant was moved to a new tube and added with 270 μl P2 buffer and 100 μl HTR reagent, and then cultivated under -20 ℃ for 5 min and then centrifuged again at 10000 g for 5 min. The supernatant was then moved to a new 2 ml tube added with the same amount of XP5 buffer and mixed upside down for 8 min. After magnetic rack adsorption, discard the residual liquid, remove the tube, add 500 μL XP5 Buffer, and mix well. Then adsorbed again with a magnetic rack, discard the residual liquid, remove the tube, add 500 μL PHB, and mix well. Then adsorbed again with a magnetic rack, discard the residual

liquid, remove the tube, add 500 μL SPW Wash Buffer, and mix well (repeat this step twice). Then the mixture was adsorbed again with a magnetic rack, discard the residual liquid, was centrifuged in the tube under 10000 g for 10 s. Then the beads were adsorbed again with a magnetic rack, discard the residual liquid, and let stand for 8 min. After that, the beads were added with 100 μL elution buffer, mixed, and let stand for 5 min. Finally, after adsorbing with a magnetic rack, the supernatant was moved to a new 1.0 ml Eppendorf tube, and total DNA was obtained for further use. The PCR reaction system was constructed.

Table S1 Main material dimensions

Material	Length/cm	Width/cm	Area/cm^2
Collector plate	10.5	5.5	57.75
Aluminum foam	6.6	5.4	35.64
GF	10.0	5.0	50.00

Table S2 Primer sequence of HRGs and MGEs

Gene	Primer sequence	Function description	Ref
chrA-F	TCCTTCGGCGGCCCTGCCGGNCARATHGC	*chrA* encodes a transporter protein involved in chromate efflux.	(Rivera et al., 2008)
chrA-R	GTAGGTGGCCAGCTGCTNGCYTCNGGNCC		
chrB-F	CCGGAATTCATGCGTGTCTGGCGAACCCTGA	*chrB* genes regulate the transcription of genes in the	(Branco and
chrB-R	CCCAAGCTTTCACTCTGCGGAAGAACGA		

		transporter protein complex.	Morais, 2013)
		The chromate reductase chrR is	(Nepple et al., 2000;
ChrR-F	AGGAACTTCTGCGTGCCCTC	the best-known of the reductases	
ChrR-R	TACGGTGACAGTGCGTTTGC	that catalyze the reduction of	Baldiris et al.,
		Cr^{6+} to Cr^{3+}.	2018).
IntI-F	CGAACGAGTGGCGGAGGGTG	MGEs such as integrons,	(Wu et
IntI-R	TACCCGAGAGCTTGGCACCCA	plasmids, and transposons play a	al.,
tnpA02-F	GGGCGGGTCGATTGAAA	key role in the transfer of	2022;
tnpA02-R	GTGGGCGGGATCTGCTT	resistance genes between	Wu et
tnpA05-F	GCCGCACTGTCGATTTTTATC	different microorganisms in the	al.,
tnpA05-R	GCGGGATCTGCCACTTCTT	environment	2023).

Table S3 Distribution percentage of EDS elements in electrode materials.

Elements	Samples					
	Cathode	Fe_3O_4-cathode	Cathode after operation	Anode	Anode with EAB-loading	Anode after operation
C	93.74%	66.85%	33.83%	6.7%	14.65%	14.35%
O	6.26%	19.97%	38.96%	47.57%	18.49%	50.92%
Fe	n.d.	13.17%	8.07%	n.d.	n.d.	0.88
Mg	n.d.	n.d.	0.44%	n.d.	0.41%	n.d.

Al	n.d.	n.d.	3.34%	37.04%	53.72%	17.56%
Cr	n.d.	n.d.	0.08%	n.d.	n.d.	0.12%
Cu	n.d.	n.d.	n.d.	n.d.	1.59%	n.d.
Zn	n.d.	n.d.	n.d.	n.d.	1.81%	n.d.
Si	n.d.	n.d.	7.16%	8.68%	9.32%	2.58%
Na	n.d.	n.d.	2.18%	n.d.	n.d.	4.55%
Ca	n.d.	n.d.	4.81%	n.d.	n.d.	n.d.
K	n.d.	n.d.	1.12%	n.d.	n.d.	0.58%
Cl	n.d.	n.d.	n.d.	n.d.	n.d.	2.67%
P	n.d.	n.d.	n.d.	n.d.	n.d.	5.81%

Table S4 SMFC power generation performance on 15-day and 30-day

Resistor (Ω)	15d-Current density (mA/m^2)	15d-Power density (mW/m^2)	30d-Current density (mA/m^2)	30d-Power density (mW/m^2)
51	448.57	37.43	485.23	42.21
100	386.53	53.84	424.57	63.47
200	296.55	62.24	357.26	90.22
510	202.88	73.52	238.08	102.02
1000	131.18	60.60	157.54	87.35
2000	75.99	40.43	95.91	64.58
5100	31.55	17.77	43.88	34.41
10000	17.01	10.13	23.95	20.09

Table S5 Performance comparison of various configurations of SMFC.

Reactor configuration	Chamber volume (L)	Output voltage （V）	Maximum power density (mW/m^2)	Reference
Single-chamber	0.72	0.33	17.3	(Li et al., 2016)

SMFC				
Single-chamber SMFC	2.16	0.297	12.1	(Yu et al., 2017)
Two-chamber SMFC	4.2	0.399	29.78	(Srivastava et al., 2019)
Single-chamber circle SMFC	0.95	0.345	24	(Yu et al., 2021)
Single-chamber SMFC	8	0.4-0.6	0.2 mW	(Yoon et al., 2023)
Single-chamber circle SMFC	n.m.	n.m.	25.51	(Wang et al., 2023)
Single-chamber SMFC	9.7	n.m.	70.4±1.4	(Dhillon et al., 2023)
Two-chamber SMFC	0.05	n.m.	71.00 ± 0.82	(Zhang et al., 2023a)
Constructed wetland MFC	38.85	0.197	12.5	(Tao et al., 2023)
Constructed wetland MFC	4.08	0.425	28.1	(Niu et al., 2023)
Plant-SMFC	0.769	0.51	46.8	(V et al., 2023)
Single-chamber circle SMFC	2	0.17	10	(Youssef et al., 2023)
Constructed wetland MFC	2.7	0.394	4468.4	(Zhang et al., 2023b)
Two-chamber SMFC	0.5	0.306	20.35	(Zhang et al., 2024)
Constructed wetland MFC	13	0.167	1.4	(Dai et al., 2024)
Plant-SMFC	1.05	0.55	8957.7	(Chen et al., 2024)
Single-chamber circle SMFC	1.6	0.4	472.52±14.2	(Zhao et al., 2024)
Single-chamber circle SMFC	1.4	0.528	178.17	(Sun and Wang, 2024)
Single-chamber SMFC	2.3	0.75	102	This study

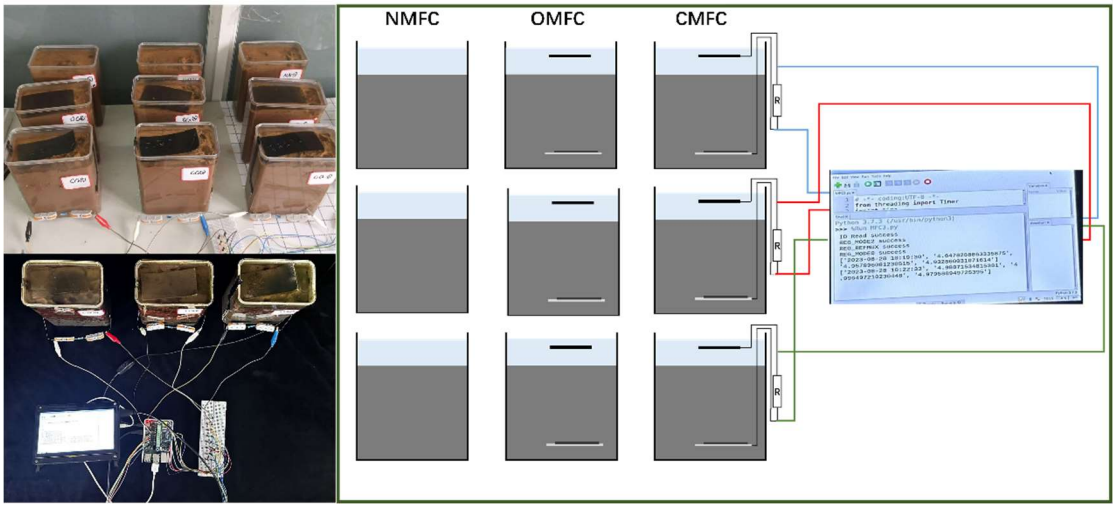

Fig. S1 SMFC structure and experimental grouping.

The left part of the picture is the SMFC photo, and the right part is the model groups. A plastic box (140.0×85.0×165.0 mm) was used as the SMFC reactor, with 1.50 kg soil and overlying water of 3.0 cm to simulate the flooded state during rice planting. The cathode was floated on the water surface while the anode was buried (about 3.0 cm from the bottom). The cathode and anode were connected to a 2000 Ω resistor using titanium wire. The water level was kept constant by daily replenishment.

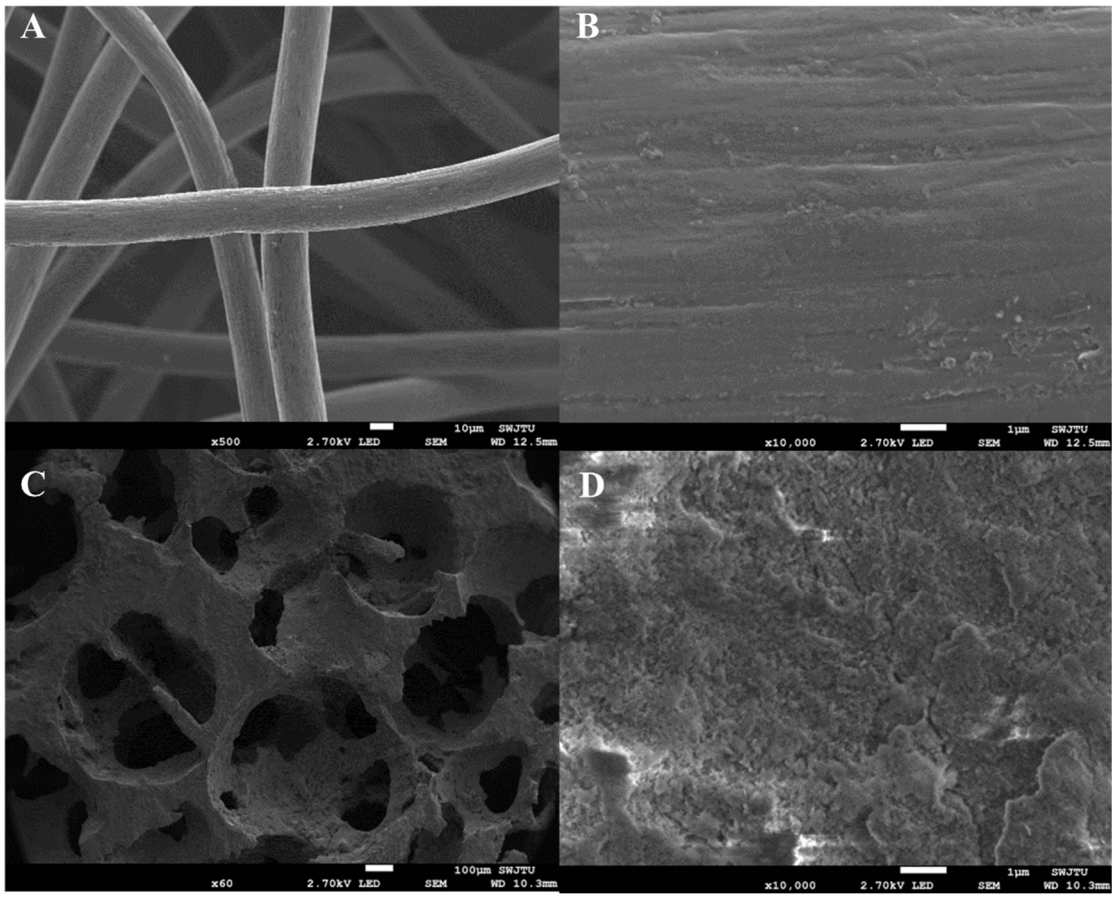

Fig. S2 Electrode material characterization. (A, B) SEM images of GF without catalyst loading; (C, D) SEM images of aluminum foam.

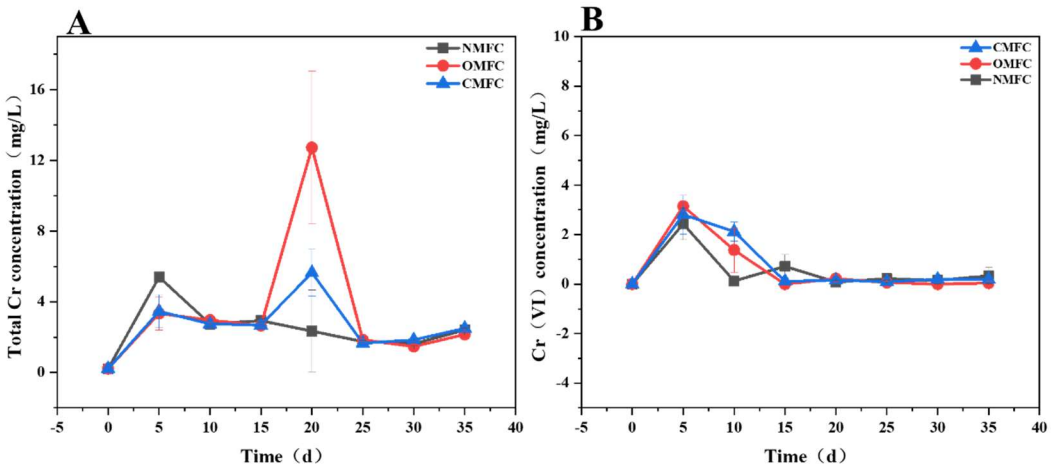

Fig. S3 Variation of (A) total chromium and (B) Cr(VI) in overlying water during SMFC operation.

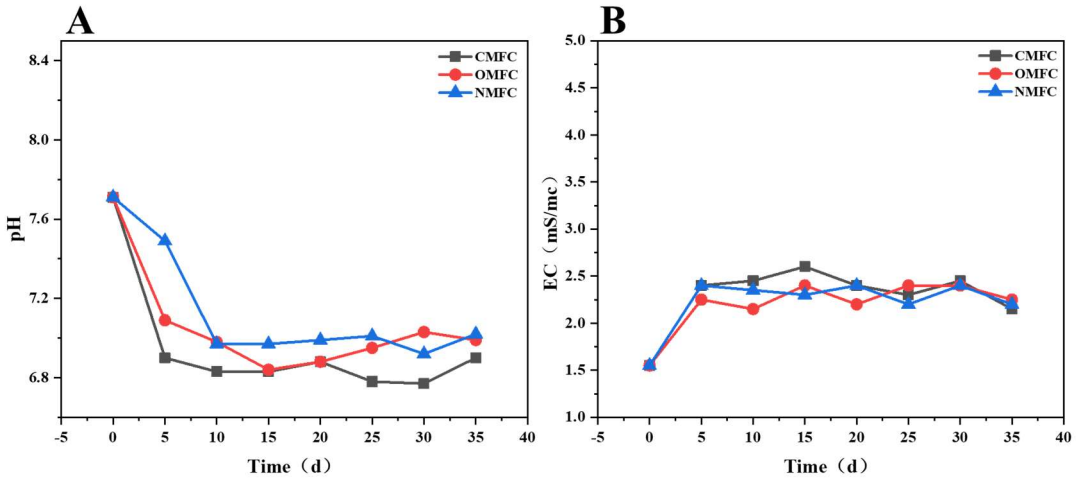

Fig. S4 pH (A), EC (B) variation curves of soil.

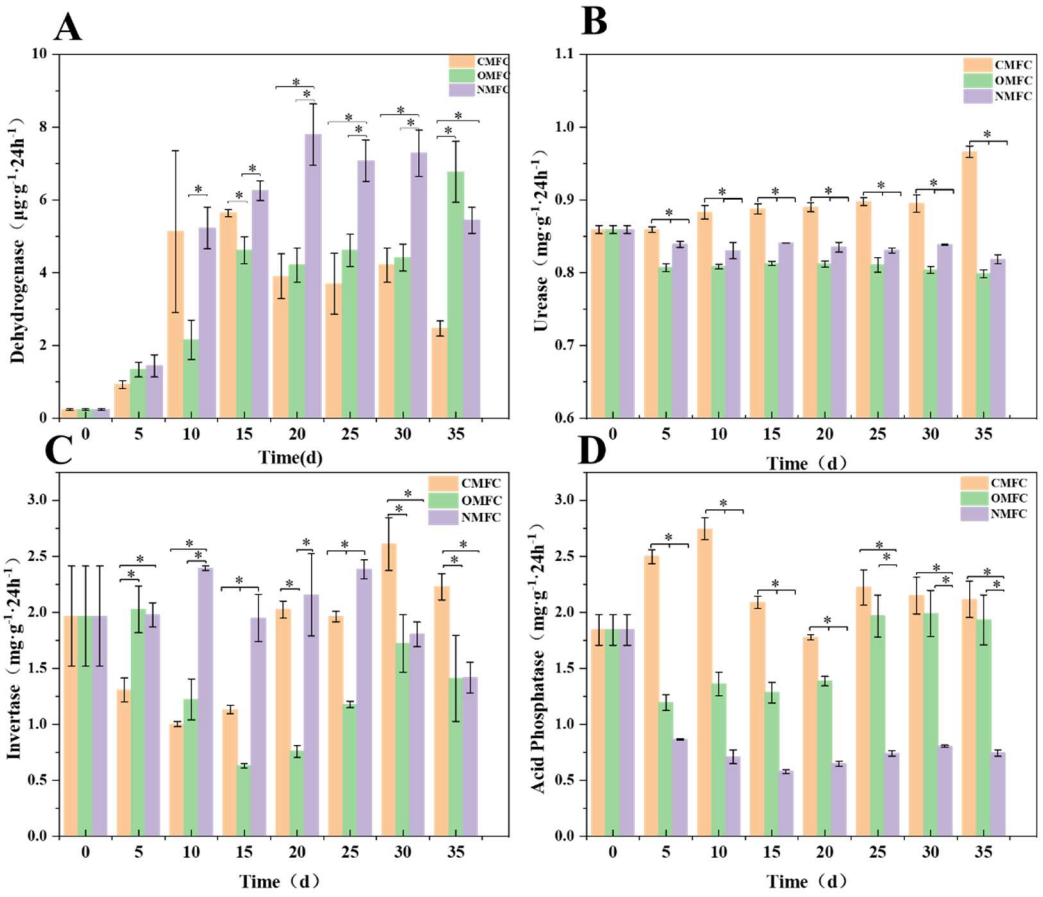

Fig. S5 Changes in soil enzyme activities during SMFC operation (A) Dehydrogenase (B) Urease (C) Invertase(D) Acid Phosphatase.

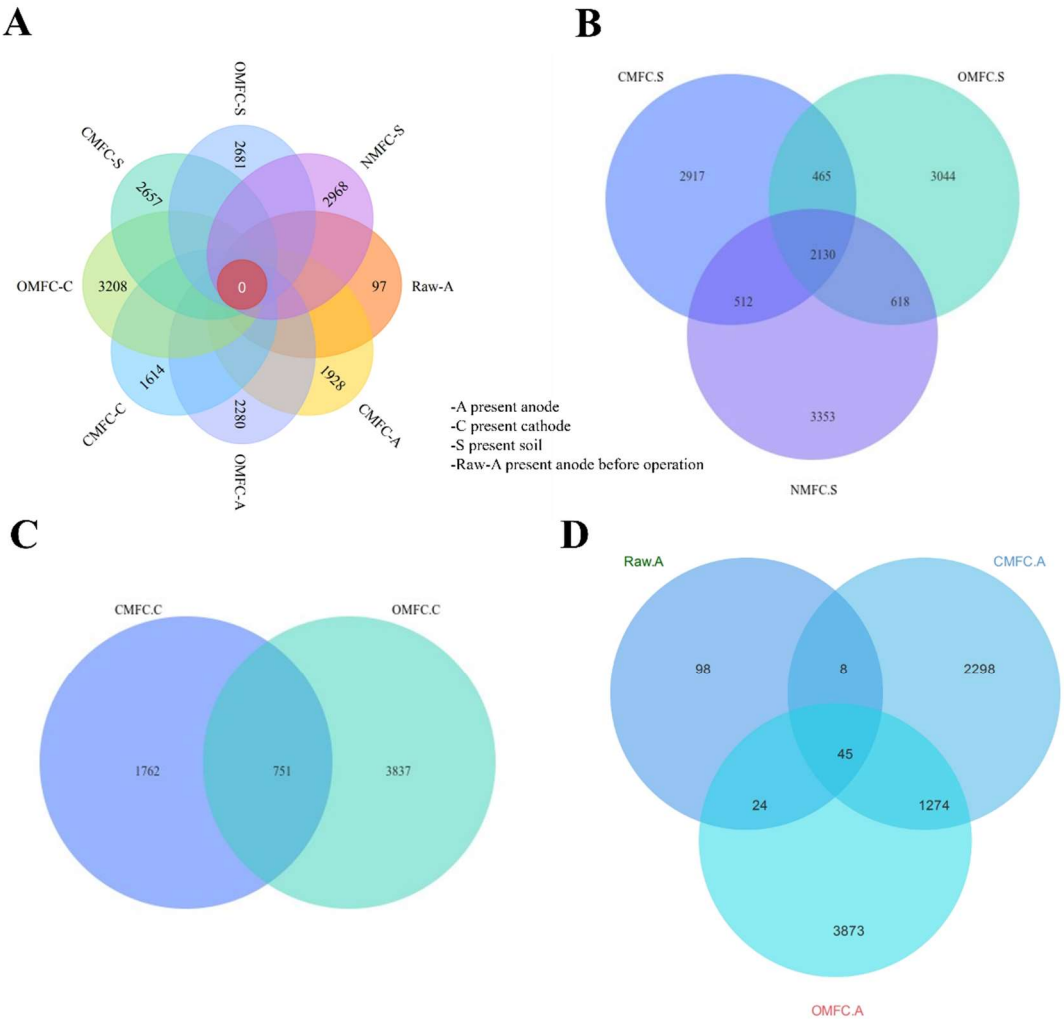

Fig. S6 Venn diagram on OTU level in different treatments

A

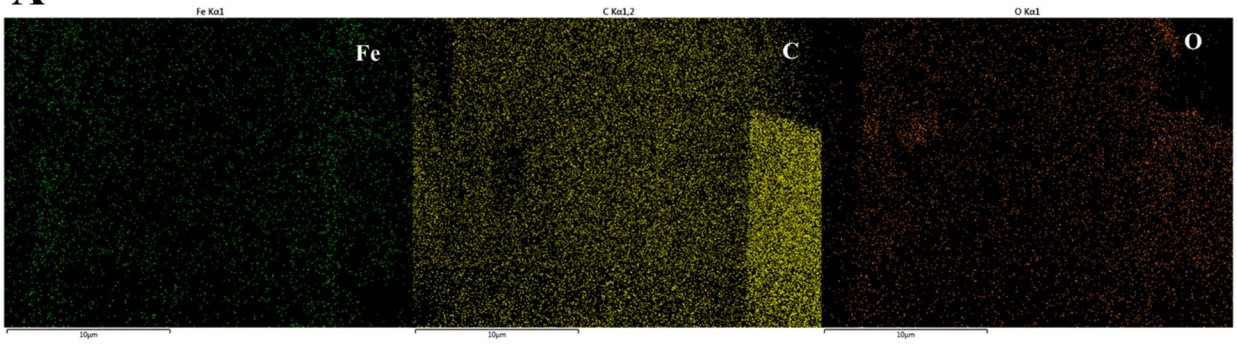

B

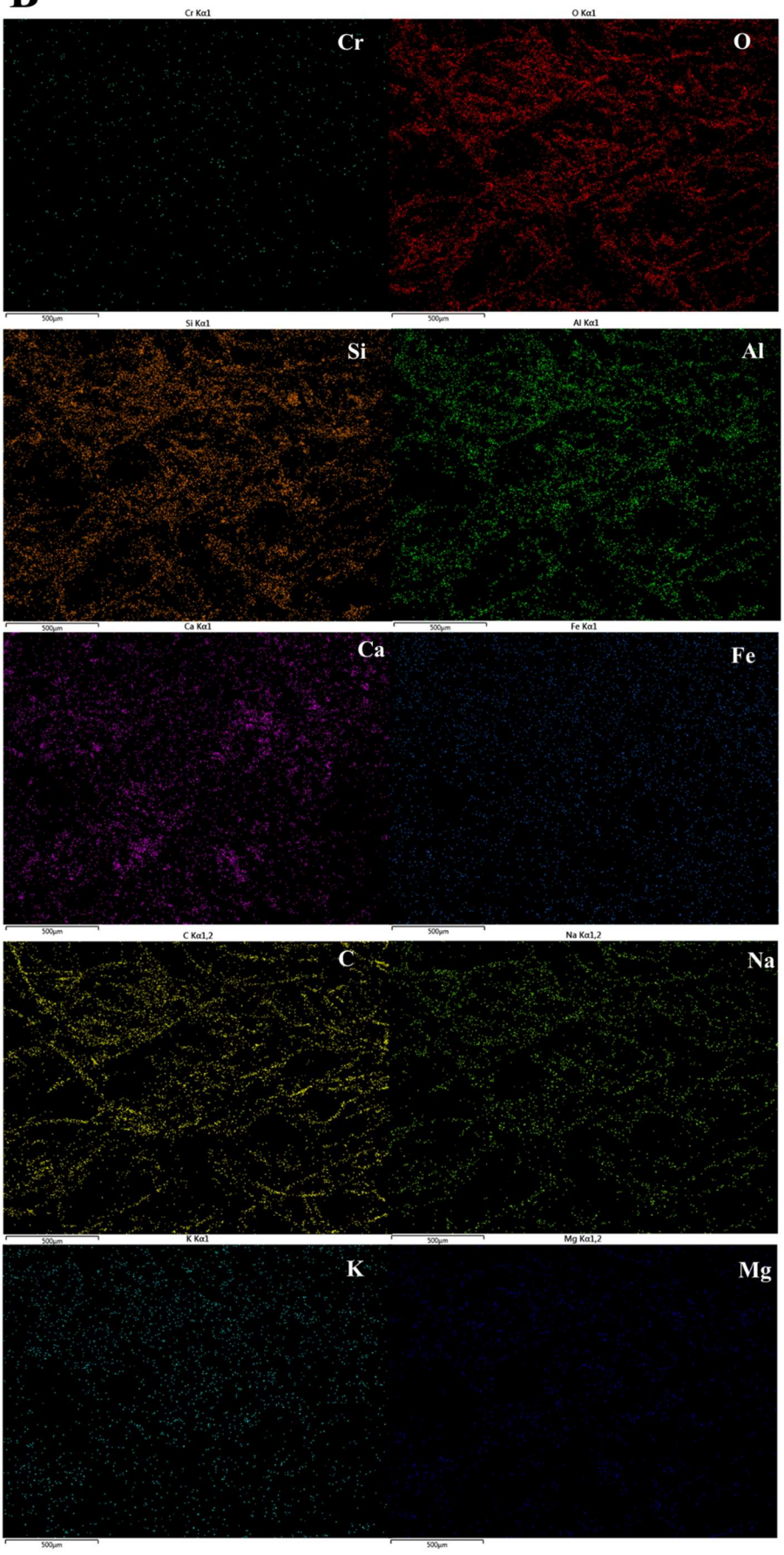
Cr Kα1
Cr
O Kα1
O
500μm
500μm
Si Kα1
Si
Al Kα1
Al
500μm
500μm
Ca Kα1
Ca
Fe Kα1
Fe
500μm
500μm
C Kα1,2
C
Na Kα1,2
Na
500μm
500μm
K Kα1
K
Mg Kα1,2
Mg
500μm
500μm

C

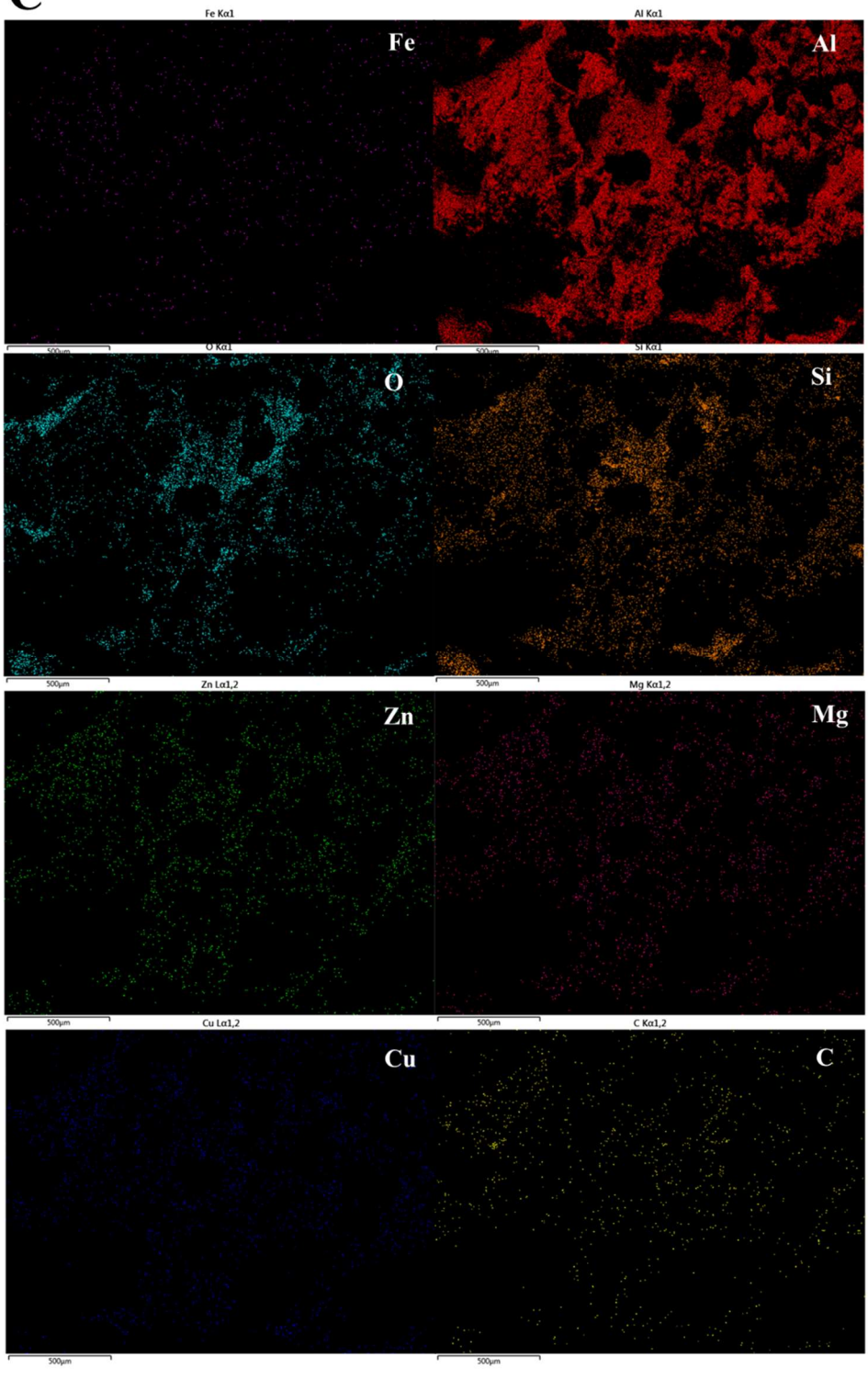
Fe Kα1
Fe
Al Kα1
Al
500μm
500μm
O Kα1
O
Si Kα1
Si
500μm
500μm
Zn Lα1,2
Zn
Mg Kα1,2
Mg
500μm
500μm
Cu Lα1,2
Cu
C Kα1,2
C
500μm
500μm

D

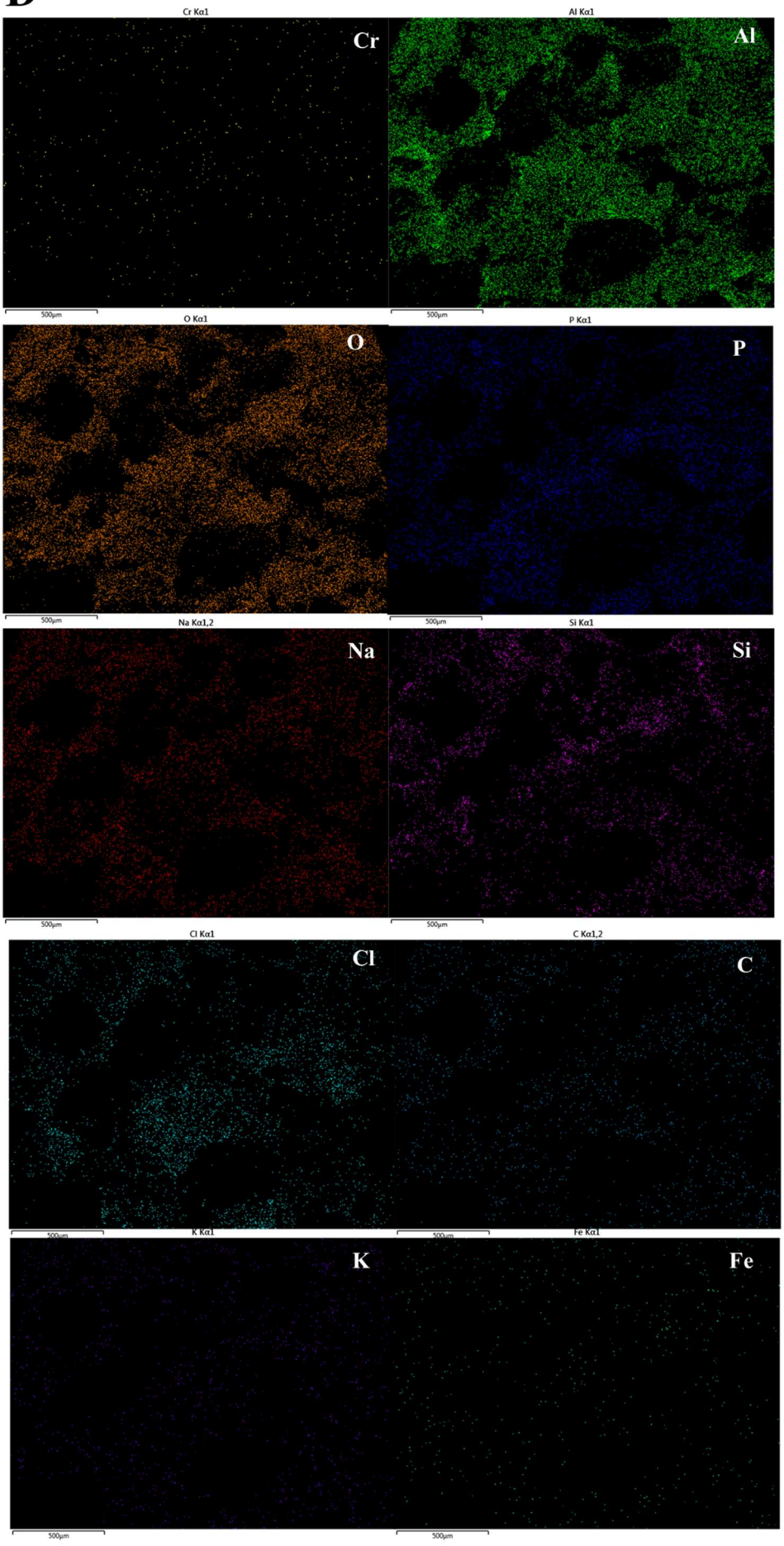
Cr Kα1
Cr
500μm
Al Kα1
Al
500μm
O Kα1
O
500μm
P Kα1
P
500μm
Na Kα1,2
Na
500μm
Si Kα1
Si
500μm
Cl Kα1
Cl
500μm
C Kα1,2
C
500μm
K Kα1
K
500μm
Fe Kα1
Fe
500μm

Fig. S7 Characterization of electrode materials before and after operation by EDS mapping. (A) EDS image of cathode loaded with Fe_3O_4; (B) EDS image of cathode after the SMFC operation; (C) EDS image of anode microorganisms; (D) EDS image of the anode after SMFC operation.

Reference:

Baldiris, R., Acosta-Tapia, N., Montes, A., Hernández, J., and Vivas-Reyes, R.: Reduction of Hexavalent Chromium and Detection of *Chromate Reductase* (*ChrR*) in *Stenotrophomonas maltophilia*, Molecules, 23, 406, https://doi.org/10.3390/molecules23020406, 2018.

Branco, R. and Morais, P. V.: Identification and Characterization of the Transcriptional Regulator ChrB in the Chromate Resistance Determinant of Ochrobactrum tritici 5bvl1, PLOS ONE, 8, e77987, https://doi.org/10.1371/journal.pone.0077987, 2013.

Chen, B., Li, L., Cai, W., and Garg, A.: Bioelectricity generation in plant microbial fuel cells: Influence of vegetation density and unsaturated soil properties, Biomass Bioenergy, 181, 107053, https://doi.org/10.1016/j.biombioe.2024.107053, 2024.

Dai, M., Li, F., Zhang, J., Shi, Q., Wu, Y., and Kong, Q.: Treatment of formaldehyde-containing wastewater and power generation by constructed wetland–microbial fuel cells enhanced by formaldehyde-degrading bacteria, J. Water Process Eng., 59, 104984, https://doi.org/10.1016/j.jwpe.2024.104984, 2024.

Dhillon, S. K., Dziegielowski, J., Kundu, P. P., and Di Lorenzo, M.: Functionalised graphite felt anodes for enhanced power generation in membrane-less soil microbial fuel cells, RSC Sustainability, 1, 310-325, https://doi.org/10.1039/D2SU00079B, 2023.

Li, X., Wang, X., Zhao, Q., Wan, L., Li, Y., and Zhou, Q.: Carbon fiber enhanced bioelectricity generation in soil microbial fuel cells, Biosensors Bioelectron., 85, 135-141, https://doi.org/10.1016/j.bios.2016.05.001, 2016.

Nepple, B. B., Kessi, J., and Bachofen, R.: Chromate reduction by *Rhodobacter sphaeroides*, J. Ind. Microbiol. Biotechnol., 25, 198-203, https://doi.org/10.1038/sj.jim.7000049, 2000.

Niu, Y., Qu, M., Du, J., Wang, X., Yuan, S., Zhang, L., Zhao, J., Jin, B., Wu, H., Wu, S., Cao, X., and Pang, L.: Effects of multiple key factors on the performance of petroleum coke-based constructed wetland-microbial fuel cell, Chemosphere, 315, 137780, https://doi.org/10.1016/j.chemosphere.2023.137780, 2023.

Rivera, S. L., Vargas, E., Ramírez-Díaz, M. I., Campos-García, J., and Cervantes, C.: Genes related to chromate resistance by *Pseudomonas aeruginosa PAO1*, Antonie Van Leeuwenhoek, 94, 299-305, https://doi.org/10.1007/s10482-008-9247-x, 2008.

Srivastava, P., Gupta, S., Garaniya, V., Abbassi, R., and Yadav, A. K.: Up to 399 mV bioelectricity generated by a rice paddy-planted microbial fuel cell assisted with a blue-green algal cathode, Environ. Chem. Lett., 17, 1045-1051, https://doi.org/10.1007/s10311-018-00824-2, 2019.

Sun, M. and Wang, C.: The application of ferrous and graphitic N modified graphene-based composite cathode material in the bio-electro-Fenton system driven by sediment microbial fuel cells to degrade methyl orange, Heliyon, 10, e24772, https://doi.org/10.1016/j.heliyon.2024.e24772, 2024.

Tao, M., Kong, Y., Jing, Z., Guan, L., Jia, Q., Shen, Y., Hu, M., and Li, Y.-Y.: Acorus calamus recycled as an additional carbon source in a microbial fuel cell-constructed wetland for enhanced nitrogen removal, Bioresour. Technol., 384, 129324, https://doi.org/10.1016/j.biortech.2023.129324, 2023.

V, K. K., K, M. m., Manju, P., and Gajalakshmi, S.: Harnessing plant microbial fuel cells for resource recovery and methane emission reduction in paddy cultivation, Environ. Chem. Lett., 294, 117545, https://doi.org/10.1016/j.enconman.2023.117545, 2023.

Wang, H., Long, X., Cao, X., Li, L., Zhang, J., Zhao, Y., Wang, D., Wang, Z., Meng, H., Dong, W., Jiang, C., Li, J., and Li, X.: Stimulation of atrazine degradation by activated carbon and cathodic effect in soil microbial fuel cell, Chemosphere, 320, 138087, https://doi.org/10.1016/j.chemosphere.2023.138087, 2023.

Wu, C., Song, X., Wang, D., Ma, Y., Ren, X., Hu, H., Shan, Y., Ma, X., Cui, J., and Ma, Y.: Effects of long-term microplastic pollution on soil heavy metals and metal resistance genes: Distribution patterns and synergistic effects, Ecotoxicol. Environ. Saf., 262, 115180, https://doi.org/10.1016/j.ecoenv.2023.115180, 2023.

Wu, Y., Wen, Q., Chen, Z., Fu, Q., and Bao, H.: Response of antibiotic resistance to the co-exposure of sulfamethoxazole and copper during swine manure composting, Sci. Total Environ., 805, 150086, https://doi.org/10.1016/j.scitotenv.2021.150086, 2022.

Yoon, Y., Kim, B., and Cho, M.: Mineral transformation of poorly crystalline ferrihydrite to hematite and goethite facilitated by an acclimated microbial consortium in electrodes of soil microbial fuel cells, Sci. Total Environ., 902, 166414, https://doi.org/10.1016/j.scitotenv.2023.166414, 2023.

Youssef, Y. A., Abuarab, M. E., Mahrous, A., and Mahmoud, M.: Enhanced degradation of ibuprofen in an integrated constructed wetland-microbial fuel cell: treatment efficiency, electrochemical characterization, and microbial community dynamics, RSC Advances, 13, 29809-29818, https://doi.org/10.1039/D3RA05729A, 2023.

Yu, B., Tian, J., and Feng, L.: Remediation of PAH polluted soils using a soil microbial fuel cell: Influence of electrode interval and role of microbial community, J. Hazard. Mater., 336, 110-118, https://doi.org/10.1016/j.jhazmat.2017.04.066, 2017.

Yu, B., Feng, L., He, Y., Yang, L., and Xun, Y.: Effects of anode materials on the performance and anode microbial community of soil microbial fuel cell, J. Hazard. Mater., 401, 123394, https://doi.org/10.1016/j.jhazmat.2020.123394, 2021.

Zhang, C., Lu, H., Wang, B., and Hu, Z.: Study on the Performance of Two-Compartment Microbial Fuel Cells Under Different Heavy Metal Concentrations, Water, Air, Soil Pollut., 235, 58, https://doi.org/10.1007/s11270-023-06869-6, 2024.

Zhang, G., Wang, Z., Liu, M., Huang, L., Jiao, Y., and Zhao, Z.: Self-Driven

Electrokinetic Remediation of Cd Contamination Soil by Using Double-Chamber Microbial Fuel Cell, J. Electrochem. Soc., 170, 075502, https://doi.org/10.1149/1945-7111/ace6fd, 2023a.

Zhang, Q., Wang, L., Xu, D., Tao, Z., Li, J., Chen, Y., Cheng, Z., Tang, X., and Wang, S.: Accelerated Pb(II) removal and concurrent bioelectricity production via constructed wetland-microbial fuel cell: Structural orthogonal optimization and microbial response mechanism, J. Water Process Eng., 56, 104287, https://doi.org/10.1016/j.jwpe.2023.104287, 2023b.

Zhao, S., Li, H., Zhou, J., Sumpradit, T., Salama, E.-S., Li, X., and Qu, J.: Simultaneous degradation of NSAIDs in aqueous and sludge stages by an electron-Fenton system derived from sediment microbial fuel cell based on a novel Fe@Mn biochar GDC, Chem. Eng. J., 482, 148979, https://doi.org/10.1016/j.cej.2024.148979, 2024.